

LPENSL-TH 05/2000

Magnetic scattering close to a ferromagnet interface: a new type of magnetic proximity effect

R. Mélin^(1,2) and D. Denaro⁽²⁾

⁽¹⁾ Centre de Recherches sur les Très basses températures (CRTBT)*
CNRS, BP 166X, 38042 Grenoble Cedex, France

⁽²⁾ Laboratoire de Physique[†], Ecole Normale Supérieure de Lyon
46 Allée d'Italie, 69364 Lyon Cedex 07, France

Abstract

The “classical” proximity effect at a ferromagnet–normal metal interface corresponds to the induction of a spin polarization in the normal metal over a length of order of the Fermi wave length. We present here another phenomenon that we also call “magnetic proximity effect”. We consider a diffusive wire of length L , doped with magnetic impurities, and connected to two ferromagnets with an antiparallel magnetization. We show that the semi classical conductance of such a contact *increases* with the length of the diffusive wire below the spin-flip length. This is reminiscent of the superconducting proximity effect where a similar scaling of the conductance is present. We also consider a diffusive wire with spin-flip scattering connected to a normal metal and a ferromagnet. In this case, only with low transparency contacts does the conductance increase with L . We solve a single impurity “spin-flip Fabry Perot interferometer” for quantum coherent multiple scattering, in which the magnetic proximity effect appears as a resonance in the conductance.

*U.P.R. 5001 du CNRS, Laboratoire conventionné avec l’Université Joseph Fourier

[†]U.M.R. CNRS 5672

1 Introduction

A ferromagnetic metal in contact with a non magnetic metal generates an induced magnetization in the otherwise non magnetic metal [1, 2, 3, 4]. The induced magnetization extends over a length scale set by the Fermi wave length. The magnetic proximity effect has been observed in various experiments [5, 6, 7, 8]. More recent experiments on granular ferromagnets have reported the existence of a coupling between the magnetic grains, mediated by a non magnetic overlayer deposited onto the grains [9]. These effects resemble the superconducting proximity effect in the sense that a ferromagnetic order parameter is induced in a non magnetic material close to a ferromagnet. In the superconducting proximity effect, superconducting correlations are generated in an otherwise normal metal close to a superconductor interface [10].

On the other hand, disorder plays a relevant role in the physics of the superconducting proximity effect. The subgap conductance of a diffusive wire connected to a superconducting reservoir scales like the resistance of the normal wire, due to coherent multiple Andreev reflections [11]. The purpose of the present article is to show that a similar phenomenon can be at work in ferromagnet junctions. More specifically, we consider in section 2 a diffusive wire connected to two ferromagnets in an antiparallel alignment, and consider the presence of magnetic impurities in the diffusive wire. The conductance of this junction scales like the Drude resistance of the diffusive wire, at least if the ferromagnet polarization is strong enough. Physically, this occurs because a spin-down electron cannot penetrate the spin-up ferromagnet. Instead, it is backscattered at the interface, undergoes spin-flip scattering in the diffusive wire, and comes back onto the interface as a spin-up electron. Increasing the size of the diffusive wire increases the amount of spin-flip scattering, and increases the junction conductance. We determine to what extend this effect persists in the presence of a partial spin polarization. On the other hand, we consider another junction with only one ferromagnet, and show that the magnetic proximity effect appears only with low transparency contacts. In section 3, we consider a quantum “spin-flip Fabry Perot” interferometer in which a single magnetic impurity is located at a given distance a away from a ferromagnet interface. We find the presence of a Fabry-Perot type resonance in the spin-flip channel as the parameter a is varied. This resonance disappears as the ferromagnet spin polarization is decreased, and can therefore be viewed as a signature of the magnetic proximity effect in the quantum coherent regime.

The article is organized as follows. Section 2 is devoted to the solution of the semi classical transport equations. Section 3 is devoted to solve the “spin-flip Fabry Perot” interferometer model. Final remarks are given in the Conclusion.

2 Transport in the semi classical regime

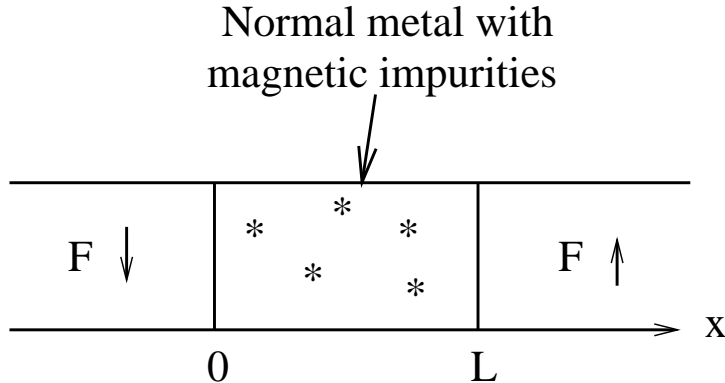


Figure 1: The “spin valve” geometry considered in section 2, consisting of a normal metal wire doped with magnetic impurities, connected to two ferromagnets with an opposite magnetization.

2.1 Boltzmann equation and boundary conditions

We start by considering spin-flip scattering in the vicinity of a ferromagnet interface via a semi classical Boltzmann equation. We assume the temperature to be above the Kondo temperature and neglect any Kondo correlation [12]. The Boltzmann equation has provided a phenomenological framework to describe the Giant Magneto Resistance (GMR) in magnetic multilayers [13, 14, 15, 16], and the interplay between spin-flip scattering and the GMR also [17, 18]. We extend these treatments to discuss the role played by the length of the paramagnetic wire connected to the ferromagnets. We restrict ourselves to a one dimensional model intended to describe two ferromagnets connected by a diffusive wire. This assumption allows to derive an exact solution, and is not really restrictive because the one dimensional physics would also hold in a quasi one dimensional geometry. We implicitly assume an effective low energy model in which the transverse degrees of freedom would be averaged out, leaving mainly the longitudinal component of the wave vector as the relevant variables.

We consider a “spin valve” geometry in which a diffusive wire doped with magnetic impurities is connected to two ferromagnets with an antiparallel magnetization (see Fig. 1). We assume the interfaces between the ferromagnets and the normal metal to be sharp, with a step function variation of the exchange field at the interface. We note $f_{R,L}^{\sigma}(E, x)$ the semi classical distribution function of right/left moving spin- σ electrons with an energy E at position x .

The Boltzmann equation in the relaxation time approximation reads

$$\frac{\partial}{\partial x} \begin{pmatrix} f_R^{\uparrow}(E, x) \\ f_L^{\uparrow}(E, x) \\ f_R^{\downarrow}(E, x) \\ f_L^{\downarrow}(E, x) \end{pmatrix} = \begin{pmatrix} -(r + r_s + r'_s) & r & r_s & r'_s \\ -r & r + r_s + r'_s & -r'_s & -r_s \\ r_s & r'_s & -(r + r_s + r'_s) & r \\ -r'_s & -r_s & -r & r + r_s + r'_s \end{pmatrix} \begin{pmatrix} f_R^{\uparrow}(E, x) \\ f_L^{\uparrow}(E, x) \\ f_R^{\downarrow}(E, x) \\ f_L^{\downarrow}(E, x) \end{pmatrix}, \quad (1)$$

where we have discarded the term involving the electric field. This is valid if the temperature of the electrodes is larger than the applied voltage, in which case the electronic gas has a temperature

identical to the one of the electrodes [19, 20]. Therefore, we should consider a finite temperature and calculate the low voltage conductance in the regime $eV \ll T$. In practise, we consider the limit $T \rightarrow 0$, and calculate the linear conductance. It is understood that $eV \ll T$, and we consider the zero temperature linear conductance of Eq. 1. The coefficients r , r_s and r'_s in Eq. 1 denote respectively the rate of backscattering without spin-flip, the rate of forward scattering with spin-flip, and the rate of backward scattering with spin-flip. The coefficients can be related to the $q = 0$ and $q = 2k_f$ components of the microscopic scattering potential (see the Appendix).

We now explicit the boundary conditions. For this purpose, let us consider an interface between a ferromagnet in the region $x < 0$ and a normal metal in the region $x > 0$, and include the effect of an interface scattering under the form of repulsive potential $H\delta(x)$ [21]. Let us first consider a spin-up electron incoming from the left ferromagnet, and denote by b^\uparrow and t^\uparrow the backscattering and transmission coefficients. The wave function in the region $x < 0$ is $\psi_L(x) = \exp(ik^\uparrow x) + b^\uparrow \exp(-ik^\uparrow x)$, and the wave function in the region $x > 0$ is $\psi_R(x) = t^\uparrow \exp(ikx)$. The matching equations are $\psi_L(0) = \psi_R(0) = \psi(0)$ and $\partial\psi_R(0)/\partial x - \partial\psi_L(0)/\partial x = (2mH/\hbar^2)\psi(0)$, from what we deduce

$$t^\uparrow = \frac{2ik^\uparrow}{i(k + k^\uparrow) - 2mH/\hbar^2}, \text{ and } b^\uparrow = \frac{i(k^\uparrow - k) + 2mH/\hbar^2}{i(k + k^\uparrow) - 2mH/\hbar^2}.$$

The probability current conservation can be verified easily: $k^\uparrow = k^\uparrow|b^\uparrow|^2 + k|t^\uparrow|^2$. The spin-up conductance is found to be $G^\uparrow = (e^2/h)|T^\uparrow|^2$, with the transmission coefficient

$$T^\uparrow = \frac{k}{k^\uparrow}|t^\uparrow|^2 = \frac{4kk^\uparrow}{(k + k^\uparrow)^2 + \left[\frac{2mH}{\hbar^2}\right]^2}. \quad (2)$$

The backscattering coefficient is $B^\uparrow = 1 - T^\uparrow$. In the spin-down sector, we obtain T^\downarrow and B^\downarrow by substituting k^\uparrow with k^\downarrow in Eq. 2. This provides the boundary conditions for the Boltzmann equation:

$$f_R^\uparrow(E, 0) = T^\downarrow f_T(E - eV) + (1 - T^\downarrow) f_L^\uparrow(E, 0) \quad (3)$$

$$f_R^\downarrow(E, 0) = T^\uparrow f_T(E - eV) + (1 - T^\uparrow) f_L^\downarrow(E, 0) \quad (4)$$

$$f_L^\uparrow(E, L) = T^\uparrow f_T(E) + (1 - T^\uparrow) f_R^\uparrow(E, L) \quad (5)$$

$$f_L^\downarrow(E, L) = T^\downarrow f_T(E) + (1 - T^\downarrow) f_R^\downarrow(E, L), \quad (6)$$

where the left and right ferromagnets are assumed to be in equilibrium and $f_T(E)$ denotes the Fermi-Dirac distribution function. We will consider T^\uparrow and T^\downarrow to be independent of energy, which amounts to considering the wave vectors k and k^\uparrow in Eq. 2 to be on the Fermi surface. Note that Eqs. 3 – 6 provide a simple form for the spin-up and spin-down currents at positions $x = 0, L$. For instance at $x = L$, we have

$$I^\uparrow(L) = T^\uparrow \frac{e}{\hbar} \int [f_R^\uparrow(E, L) - f_T(E)] dE \quad (7)$$

$$I^\downarrow(L) = T^\downarrow \frac{e}{\hbar} \int [f_R^\downarrow(E, L) - f_T(E)] dE. \quad (8)$$

The Boltzmann equation Eq. 1 and the boundary conditions Eqs. 3– 6 lead to eight equations for eight variables $f_{R,L}^{\uparrow,\downarrow}(E, x = 0, L)$. We now solve these equations and discuss their physics.

2.2 Solution of the Boltzmann equation

The Boltzmann equation is block diagonalized by changing variables to the charge and spin combinations $X_{R,L} = f_{R,L}^{\uparrow} + f_{R,L}^{\downarrow}$ and $Y_{R,L} = f_{R,L}^{\uparrow} - f_{R,L}^{\downarrow}$. We find

$$\frac{\partial}{\partial x} \begin{pmatrix} X_R \\ X_L \end{pmatrix} = \frac{1}{l} \begin{pmatrix} -1 & 1 \\ -1 & 1 \end{pmatrix} \begin{pmatrix} X_R \\ X_L \end{pmatrix}, \text{ and } \frac{\partial}{\partial x} \begin{pmatrix} Y_R \\ Y_L \end{pmatrix} = \begin{pmatrix} -a & b \\ -b & a \end{pmatrix} \begin{pmatrix} Y_R \\ Y_L \end{pmatrix}, \quad (9)$$

with $l = 1/(r + r'_s)$ the mean free path, and $a = r + 2r_s + r'_s$, $b = r - r'_s$. The 2×2 block equations can be easily integrated to obtain

$$\begin{pmatrix} X_R(L) \\ X_L(L) \end{pmatrix} = \begin{pmatrix} 1-x & x \\ -x & 1+x \end{pmatrix} \begin{pmatrix} X_R(0) \\ X_L(0) \end{pmatrix}, \quad (10)$$

with $x = L/l$. Similarly,

$$\begin{pmatrix} Y_R(L) \\ Y_L(L) \end{pmatrix} = \hat{T} \begin{pmatrix} X_R(0) \\ X_L(0) \end{pmatrix}, \text{ with } \hat{T} = \begin{pmatrix} t & u \\ -u & \bar{t} \end{pmatrix}, \quad (11)$$

where $t = \cosh(\lambda L) - \alpha \sinh(\lambda L)$, $\bar{t} = \cosh(\lambda L) + \alpha \sinh(\lambda L)$, and $u = \beta \sinh(\lambda L)$. We used the notation $\alpha = a/\lambda$, $\beta = b/\lambda$, and $\lambda = \sqrt{a^2 - b^2}$. Next, we combine the boundary conditions Eqs. 3– 6 to Eq. 10 to obtain an expression for $f_R^{\uparrow}(E, 0) - f_R^{\downarrow}(E, 0)$ and $f_L^{\uparrow}(E, 0) - f_L^{\downarrow}(E, 0)$ as a function of $f_R^{\uparrow}(E, L)$ and $f_R^{\downarrow}(E, L)$. Once injected into Eq. 11, these relations lead to

$$\begin{aligned} \hat{M} \begin{pmatrix} f_R^{\uparrow}(E, L) \\ f_R^{\downarrow}(E, L) \end{pmatrix} &= 2f_T(E - eV)\hat{T} \begin{pmatrix} T^{\uparrow} + T^{\downarrow} - 2T^{\uparrow}T^{\downarrow} \\ T^{\uparrow} + T^{\downarrow} \end{pmatrix} \\ &- f_T(E) \left\{ (T^{\uparrow} + T^{\downarrow})\hat{T} \begin{pmatrix} 2(T^{\uparrow} + T^{\downarrow} - T^{\uparrow}T^{\downarrow} - 1) - x(T^{\uparrow} + T^{\downarrow} - 2T^{\uparrow}T^{\downarrow}) \\ -2 + T^{\uparrow} + T^{\downarrow} - x(T^{\uparrow} + T^{\downarrow}) \end{pmatrix} \right. \\ &\left. - (T^{\uparrow} - T^{\downarrow})^2 \begin{pmatrix} 0 \\ 1 \end{pmatrix} \right\}. \end{aligned} \quad (12)$$

The matrix \hat{M} appearing in the left hand side of Eq. 12 is

$$\hat{M} = \hat{T} \begin{pmatrix} A^{\uparrow} & A^{\downarrow} \\ B^{\uparrow} & B^{\downarrow} \end{pmatrix} + (T^{\uparrow} - T^{\downarrow}) \begin{pmatrix} -1 & 1 \\ -1 + T^{\uparrow} & 1 - T^{\downarrow} \end{pmatrix}, \quad (13)$$

with the coefficients

$$A^{\uparrow} = 3T^{\uparrow} - 4T^{\uparrow}T^{\downarrow} + T^{\downarrow} - 2(T^{\uparrow})^2 + 2(T^{\uparrow})^2T^{\downarrow} + xT^{\uparrow} [T^{\uparrow} - 2T^{\uparrow}T^{\downarrow} + T^{\downarrow}] \quad (14)$$

$$B^{\uparrow} = 3T^{\uparrow} + T^{\downarrow} - (T^{\uparrow})^2 - T^{\uparrow}T^{\downarrow} + x [(T^{\uparrow})^2 + T^{\uparrow}T^{\downarrow}]. \quad (15)$$

The expression of A^{\downarrow} is obtained by exchanging T^{\uparrow} and T^{\downarrow} in Eq. 14. Similarly, B^{\downarrow} is obtained from B^{\uparrow} by exchanging T^{\uparrow} and T^{\downarrow} in Eq. 15.

2.3 Fully polarized limit

We first consider the solution Eq. 12 in the case of fully polarized ferromagnets with high transparency contacts: $H = 0$, $k^\downarrow = T^\downarrow = 0$, $k^\uparrow = k$, leading to $T^\uparrow = 1$. In this limit, only a spin-up current can enter the ferromagnet at $x = L$. This is expected on physical grounds, and it can be verified explicitly on the form Eq. 8 of the spin-down current. The total current is found to be

$$I = \frac{e}{h} \int dE \frac{2\sqrt{a-b} \sinh(\lambda L) [f_T(E - eV) - f_T(E)]}{\sqrt{a+b} + 2\sqrt{a-b} \sinh(\lambda L) + \sqrt{a+b} \cosh(\lambda L) + (L/l)\sqrt{a-b} \sinh(\lambda L)}. \quad (16)$$

We consider the situation $r'_s = 0$ and $r_s \ll r$, in which case the elastic mean free path $l \sim 1/r$ is much below the spin-flip length $l_{sf} = 1/\lambda \sim 1/(2\sqrt{rr_s})$. If L is small compared to l_{sf} , the conductance $G \sim 2\frac{e^2}{h}r_sL$ increases linearly with the length of the diffusive wire. In terms of the Drude resistance of the intermediate normal wire $R_N = h/(2e^2) \times (L/l)$ [22], we have $G \sim (2e^2/h)^2 l r_s R_N$. This form of the conductance is reminiscent of the conductance of a wire connected to a superconductor by a tunnel junction, also proportional to the normal state resistance of the wire [11]. We are lead to consider that our system realizes a ferromagnetic analog of the superconducting proximity effect [11, 23, 24, 25, 26, 27, 28, 29, 30, 31, 32]. In the superconducting proximity effect, disorder in the normal metal allows multiple Andreev reflections. In our system, spin-up electrons cannot penetrate the spin-down ferromagnet. These electrons are reflected at the interface, can change their spin in the presence of magnetic scattering, and penetrate the ferromagnet as a spin-down electron.

It is instructive to notice that the length scale controlling the cross-over from a current increasing linearly with the length L of the intermediate wire, and a current decreasing like $1/L$, is set by $2\sqrt{a+b} \sim x\sqrt{a-b}\lambda L$, leading to the cross-over length $L \sim l_{sf} \sim 1/(2\sqrt{rr_s})$, equal to the spin-flip length. The current is controlled solely by the length scale l_{sf} and *not* by the elastic mean free path l . This shows the drastic role played by spin-flip scattering in such junctions. This also shows that multiple spin flip scatterings play a relevant role. If the physics were controlled by a single spin flip scattering, the cross over length would be of order $1/r_s$, inverse proportional to the concentration of spin flip scatterers. On the contrary, the relevant length is $l_{sf} \ll 1/r_s$. This is because the elastic mean free path $l \sim 1/r$ is much below the average spacing $\sim 1/r_s$ between the magnetic impurities. The electrons hit several times a given magnetic impurity. The electrons can also hit the ferromagnet interface a large number of times, until tunneling into the ferromagnet is possible. With low transparency contacts, even an electron with an aligned spin can be backscattered at the interface.

2.4 Spin polarization profile

The spin polarization profile in the diffusive wire can be calculated in a straightforward fashion from the solution of the Boltzmann equation. Once we know the distribution functions at one extremity of the wire, we can use Eqs. 9 to propagate the solution to an arbitrary point. The resulting spin

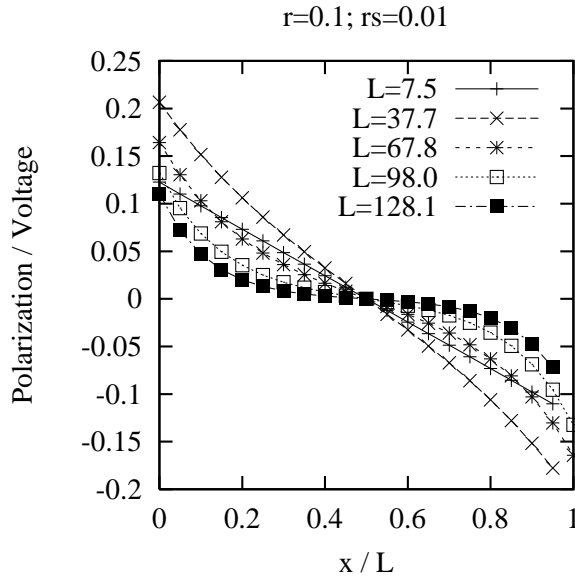


Figure 2: Spin polarization profile inside the diffusive conductor, with $r = 0.1$, $r_s = 0.01$, and increasing values of L . The spin polarization is normalized to the applied voltage, and the coordinate along the wire is normalized to the total length. We have $1/\lambda = 15.8$. It is visible that a magnetization is induced in the normal wire. This is why we call this effect a “magnetic proximity effect”.

polarization inside the wire is proportional to the applied voltage, and is shown on Fig. 2 for various values of L . With the length L of the diffusive wire larger than the spin-flip length $1/\lambda$, the spin polarization decreases to zero in the middle of the wire, over the length scale $1/\lambda$. This plateau is not present if the length of the diffusive wire is smaller than $1/\lambda$, in which case the conductance is increasing with the length of the diffusive wire.

2.5 Effect of a partial spin polarization

Now, we consider the effect of a partial spin polarization in the ferromagnet. It is expected on physical grounds that a decreasing spin polarization tends to suppress the regime in which the conductance increases with the length of the diffusive wire because such a regime is clearly absent in the spin unpolarized case. This is visible on Fig. 3 where we plotted the conductance as a function of the length of the diffusive wire for decreasing spin polarizations. With an arbitrary polarization, there exists a critical length scale L_c such that the conductance increases with L below L_c , and decreases with L above L_c . There exists also a critical value of T^\downarrow such that $L_c = 0$ if $T^\downarrow > T_c^\downarrow$. To illustrate this, we have shown on Fig. 4 the variations of the critical length L_c as a function of the parameter T^\downarrow . When T^\downarrow increases, L_c decreases: the maximum in $G(L)$ occurs for a smaller L_c . When T^\downarrow is above a critical value T_c^\downarrow , the conductance decreases monotonically with L .

We now describe the effect of a partial spin polarization on the basis of a small- T^\downarrow expansion.

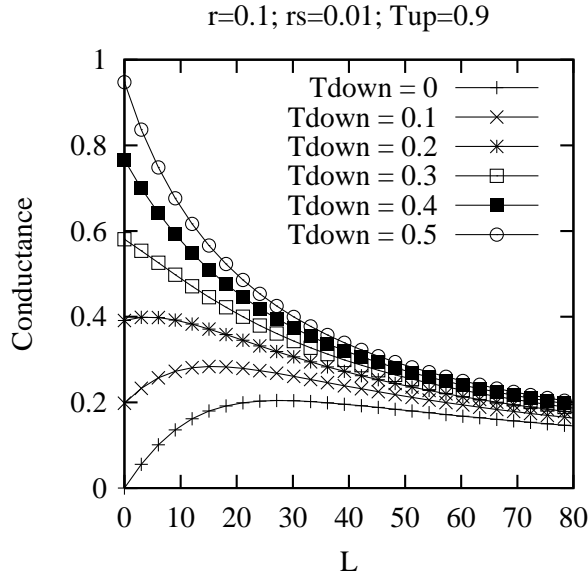


Figure 3: Variations of the conductance as a function of the length L of the diffusive wire, with decreasing spin polarizations $T^\downarrow = 0, 0.1, 0.2, 0.3, 0.4, 0.5$, and the parameters $T^\uparrow = 0.9$, $r = 0.1$ and $r_s = 0.01$. With a strong spin polarization, the conductance increases with L below L_c . With a weak spin polarization, the conductance decreases monotonically with L ($L_c = 0$).

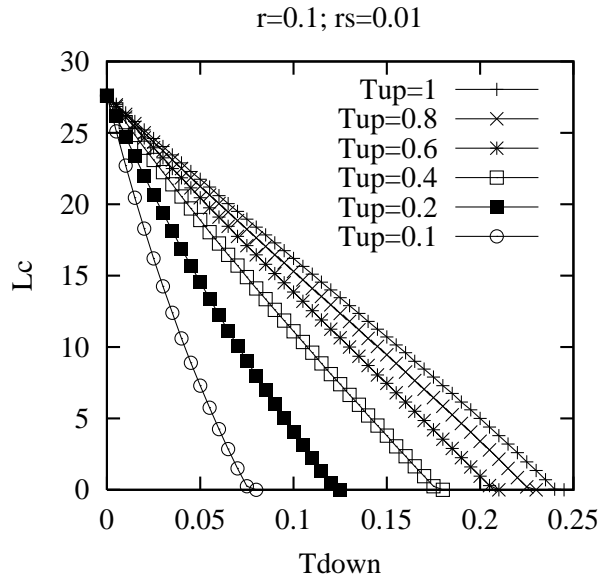


Figure 4: Variations of L_c as a function of T^\downarrow , with increasing spin polarizations $T^\uparrow = 0.1, 0.2, 0.4, 0.6, 0.8, 1$, and the parameters $r = 0.1$ and $r_s = 0.01$. With a given T^\uparrow , the curve $L_c(T^\downarrow)$ separates two regions: (i) small- L , small- T^\downarrow : the conductance increases with L ; and (ii) large- L , large- T^\downarrow : the conductance decreases with L .

The strategy is to express the current to order L and determine whether the conductance increases or decreases with L . We expand the current to first order in the two parameters $K = \lambda L$ and $x = L/l$, and retain the coefficients of this expansion to leading order in T^\downarrow . It is first instructive to carry out the expansion with $L = 0$, and therefore $K = x = 0$. It is visible on Eqs. 7, 8 that a prefactor T^\uparrow enters the spin-up current, and a prefactor T^\downarrow enters the spin-down current. We should then express $f_R^\uparrow(E, L)$ to first order in T^\downarrow while $f_R^\downarrow(E, L)$ should be expressed to order $(T^\downarrow)^0$. The spin-up and spin-down channels appear to play an asymmetric role. Nevertheless, the final expression of the conductance is identical in the spin-up and spin-down channels. An intermediate step in the calculation of $f_R^\uparrow(E, L)$ is the derivation of $\text{Det}\hat{M}$ to order T^\downarrow (see Eq. 13):

$$\text{Det}\hat{M} = -4(T^\uparrow)^3 \left\{ 1 - T^\downarrow \left(\frac{2T^\uparrow - 1}{T^\uparrow} \right) \right\},$$

leading to an identical current in both spin channels:

$$I^\uparrow = I^\downarrow = T^\downarrow \frac{e}{h} \int [f_T(E - eV) - f_T(E)] dE.$$

Now we consider a diffusive wire with a finite length L , and expand the current to first order in x and K , and to leading order in T^\downarrow . The determinant of the matrix \hat{M} in Eq. 12 is found to be

$$\text{Det}\hat{M} = -4(T^\uparrow)^3 \left\{ 1 - T^\downarrow \left(\frac{2T^\uparrow - 1}{T^\uparrow} \right) \right\} - 4(T^\uparrow)^2(\alpha - \beta)(2 - T^\uparrow)K - 4x(T^\uparrow)^2T^\downarrow.$$

Next we expand the spin-up current to order L to obtain

$$I^\uparrow = \frac{-4(T^\uparrow)^3}{\text{Det}\hat{M}} (T^\downarrow - (\alpha - \beta)K) \simeq T^\downarrow \left[1 + K \frac{\alpha - \beta}{T^\downarrow} - x \frac{T^\downarrow}{T^\uparrow} \right].$$

If T^\downarrow is small, the current increases with L while it decreases with L if T^\downarrow is large. The transition between these two behaviors is obtained for $T_c^\downarrow = \sqrt{(2r_s/r)T^\uparrow}$, compatible with the behavior shown on Fig. 4.

2.6 Replacement of one of the ferromagnets by a normal metal

We now consider the situation where we replace the left-hand-side ferromagnet on Fig. 1 by a normal metal. In the presence of high transparency contacts, the conductance of this junction is of order e^2/h in the absence of diffusion while it is of order $(e^2/h)T^\downarrow$ in the spin valve geometry on Fig. 1. Replacing one of the ferromagnets by a normal metal is expected to compete with the magnetic proximity effect. The boundary conditions appropriate to describe this situation are

$$f_R^\uparrow(E, 0) = T f_T(E - eV) + (1 - T) f_L^\uparrow(E, 0) \quad (17)$$

$$f_R^\downarrow(E, 0) = T f_T(E - eV) + (1 - T) f_L^\downarrow(E, 0) \quad (18)$$

$$f_L^\uparrow(E, L) = T^\uparrow f_T(E) + (1 - T^\uparrow) f_R^\uparrow(E, 0) \quad (19)$$

$$f_L^\downarrow(E, L) = T^\downarrow f_T(E) + (1 - T^\downarrow) f_R^\downarrow(E, 0), \quad (20)$$

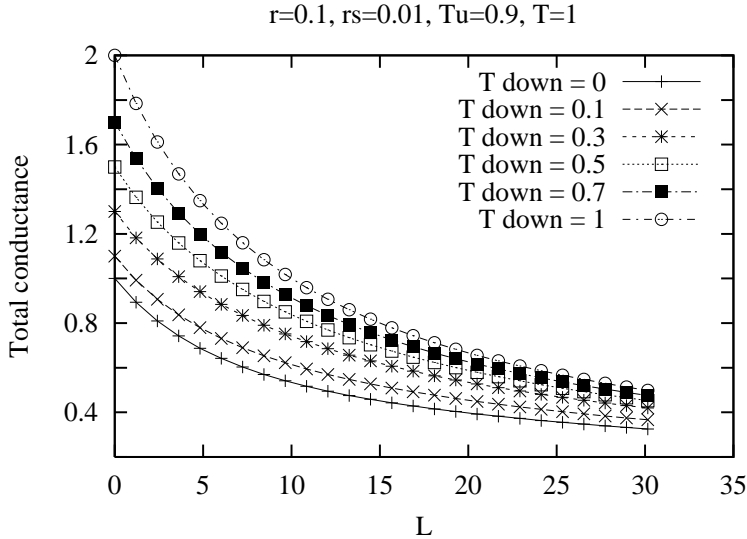


Figure 5: Conductance of the junction with a diffusive wire connected to a normal metal and a ferromagnet, with high transparency contacts: $T = T^\uparrow = 1$. It is visible that the conductance decreases monotonically with the length of the diffusive wire.

that should be solved together with Eqs. 9. The solution is found to be

$$\hat{N} \begin{pmatrix} f_R^\uparrow(E, L) \\ f_R^\downarrow(E, L) \end{pmatrix} = \begin{pmatrix} (T^\uparrow + T^\downarrow)(1 - T + xT) \\ (T^\uparrow - T^\downarrow)(u + t(1 - T)) \end{pmatrix} f_T(E) + 2T \begin{pmatrix} 1 \\ 0 \end{pmatrix} f_T(E - eV),$$

with

$$\hat{N} = \begin{pmatrix} C^\uparrow & C^\downarrow \\ D^\uparrow & -D^\downarrow \end{pmatrix},$$

and

$$C^\uparrow = T + T^\uparrow - TT^\uparrow + xTT^\uparrow \quad (21)$$

$$D^\uparrow = \bar{t} - u(1 - T) - (1 - T^\uparrow)(t(1 - T) + u). \quad (22)$$

We have plotted on Fig. 5 the conductance of the junction with high transparency contacts, where it is visible that the conductance decreases monotonically with the length of the diffusive wire.

Now, reducing the contact transparency restores a regime in which the conductance increases with the size of the diffusive wire. This is visible on Fig. 6 where we used $T = 0.01$ and $T^\uparrow = 1$. Again, the magnetic proximity effect is obtained for the smallest values of T^\downarrow (with strongly polarized magnets).

3 Quantum coherent transport: a single magnetic impurity “spin-flip Fabry Perot interferometer”

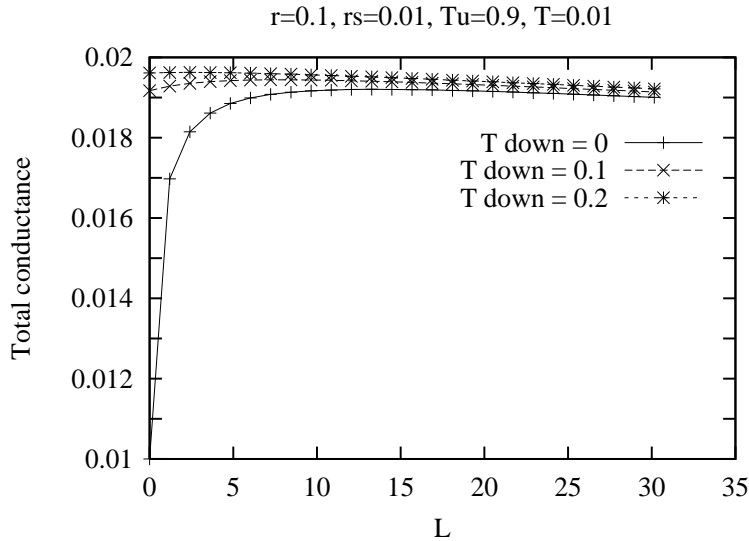


Figure 6: Conductance of the junction with a diffusive wire connected to a normal metal and a ferromagnet, with low transparency contacts: $T = 0.01$, and $T^\uparrow = 1$. A regime with a conductance increasing with the length of the diffusive wire is visible for small values of the parameter T^\downarrow .

3.1 Matching equations

We now consider a single magnetic impurity at $x = 0$ in a normal metal, in the presence of a normal metal – ferromagnet interface at $x = a$ (see Fig. 7). This purpose of this calculation is to study a model in which the interplay between the multiple reflections and phase coherence is treated exactly, and to determine to what extend the quantum mechanical model confirms the picture arising from the semi classical treatment. Not surprisingly, we find that the quantum model behaves like a Fabry Perot interferometer, in which the magnetic proximity effect appears as a resonance in the conductance. We neglect the Kondo effect because we want to describe a situation in which the

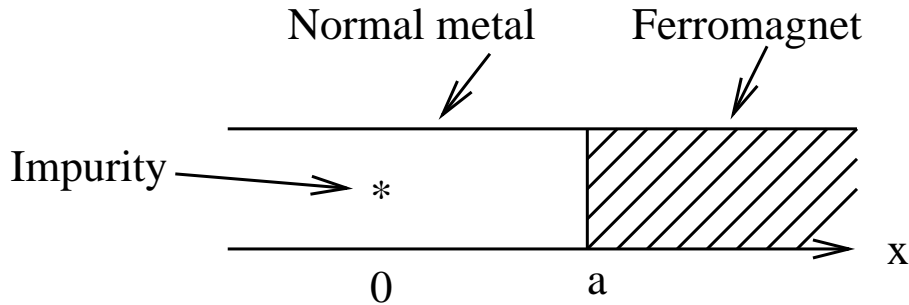


Figure 7: The system considered in section 3. The impurity is in the normal metal at a distance a away from the ferromagnet. We have represented a quasi one dimensional geometry while the calculation is made in a one dimensional geometry.

temperature is above the Kondo temperature. The conduction electrons are scattered through the Hamiltonian $\mathcal{H} = V_0 + V_1 \mathbf{S}_i \cdot \mathbf{s}$, where \mathbf{S}_i is the impurity spin and \mathbf{s} the spin of the conduction electron, and we further assume a single channel geometry. This type of model has been used by Zhu and Wang [33] to model the effect of a magnetic impurity close to a normal metal – superconductor interface. The spin-up and spin-down wave functions are grouped in a two-component spinor $\hat{\psi}(x)$. Clearly, the impurity couples the spin-up and spin-down wave functions. The matching of the wave function at the impurity site reads

$$\hat{\psi}(0^+) = \hat{\psi}(0^-), \text{ and } \frac{\partial \hat{\psi}}{\partial x}(0^+) - \frac{\partial \hat{\psi}}{\partial x}(0^-) = \frac{2m}{\hbar^2} [\lambda \hat{1} + \mu \hat{\sigma}_x] \hat{\psi}(0), \quad (23)$$

with $\lambda = V_0 - V_1/4$ and $\mu = V_1/2$. The matching of the wave function at the ferromagnet boundary reads

$$\hat{\psi}(a^+) = \hat{\psi}(a^-), \text{ and } \frac{\partial \hat{\psi}}{\partial x}(a^+) - \frac{\partial \hat{\psi}}{\partial x}(a^-) = \frac{2m}{\hbar^2} H \hat{\psi}(a), \quad (24)$$

where we included a repulsive interface potential $H\delta(x - a)$ at the normal metal – ferromagnet interface. Eqs. 23, 24 generate eight constraints, for a set of eight transmission coefficients.

This calculation amounts to a resummation to all orders of a series of diagrams in which a conduction electron scatters onto the impurity, scatters back onto the interface, scatters again onto the impurity, ... (see Fig. 8 (a)). Note that the diagram with a hole in the intermediate state shown on Fig. 8 (b) generates another series which is not included in the calculation. If one wanted to describe the Kondo effect close to a ferromagnet interface, it would be crucial to incorporate the diagram on Fig. 8 (b), as well as inserting the interface scattering in this diagram.

3.2 Scattering in the total spin $S^z = 0$ sectors

3.2.1 Incoming electron with a spin-up

We first consider a spin-up electron incoming on the interface while the impurity is supposed to have initially a spin down. The wave functions are

$$\hat{\psi}_{i\downarrow}^{e\uparrow}(x) = \begin{pmatrix} 1 \\ 0 \end{pmatrix} e^{ikx} + \begin{pmatrix} b_{i\downarrow}^{e\uparrow \rightarrow e\uparrow} \\ b_{i\downarrow}^{e\uparrow \rightarrow e\downarrow} \end{pmatrix} e^{-ikx} \text{ if } x < 0. \quad (25)$$

$$\hat{\psi}_{i\downarrow}^{e\uparrow}(x) = \begin{pmatrix} \alpha \\ \alpha' \end{pmatrix} e^{ikx} + \begin{pmatrix} \beta \\ \beta' \end{pmatrix} e^{-ikx} \text{ if } 0 < x < a. \quad (26)$$

$$\hat{\psi}_{i\downarrow}^{e\uparrow}(x) = t_{i\downarrow}^{e\uparrow \rightarrow e\uparrow} \begin{pmatrix} 1 \\ 0 \end{pmatrix} e^{ik^\uparrow x} + t_{i\downarrow}^{e\uparrow \rightarrow e\downarrow} \begin{pmatrix} 0 \\ 1 \end{pmatrix} e^{ik^\downarrow x} \text{ if } x > a, \quad (27)$$

where k^\uparrow and k^\downarrow denote the spin-up and spin-down Fermi wave vectors in the ferromagnet. In the notation of the transmission coefficients, the superscript denotes the initial and final spin orientations of the conduction electron while the subscript denotes the initial orientation of the impurity. The

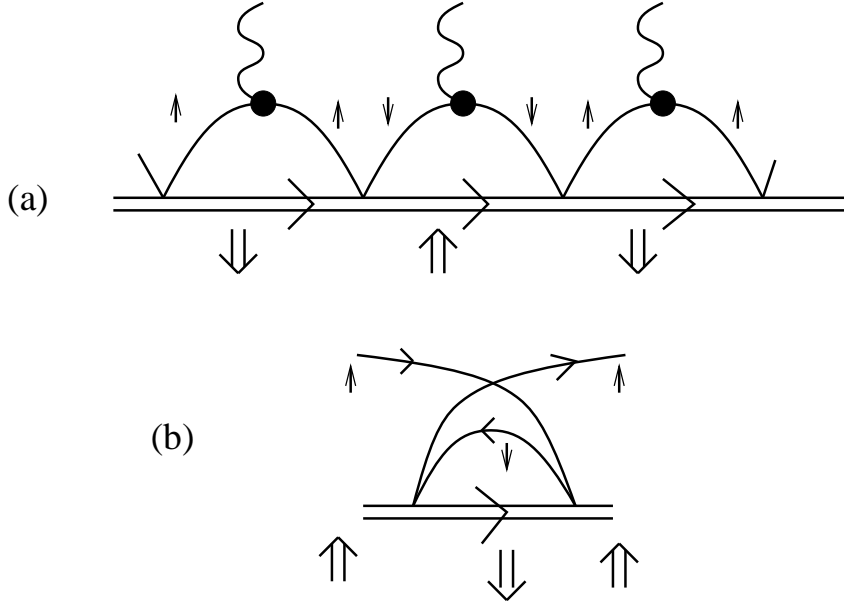


Figure 8: (a) The processes included in the Landauer calculation. The wavy lines indicate the scattering at the interface; and (b) A process with a hole in the intermediate state, not included in the calculation.

solution of the matching equations is straightforward, and we find the transmission coefficients

$$t_{i\downarrow}^{e\uparrow \rightarrow e\uparrow} = \frac{1}{\mathcal{D}A^\uparrow} [\bar{A}(1+iz)X^\downarrow + AizY^\downarrow] \quad (28)$$

$$t_{i\downarrow}^{e\uparrow \rightarrow e\downarrow} = -\frac{1}{\mathcal{D}A^\downarrow} iz' [\bar{A}X^\uparrow + AY^\uparrow]. \quad (29)$$

We used the notation $X^\sigma = \frac{1}{2} + iZ + \frac{Z}{2Z^\sigma}$, $Y^\sigma = \frac{1}{2} - (iZ + \frac{Z}{2Z^\sigma})$, $A = \exp(ika)$, $A^\sigma = \exp(ik^\sigma a)$. The dimensionless scattering potentials in Eqs. 28, 29 are $z = m\lambda/(\hbar^2 k)$ and $z' = m\mu/(\hbar^2 k)$ at the impurity site, and $Z = mH/(\hbar^2 k)$, $Z^\sigma = mH/(\hbar^2 k^\sigma)$ at the normal metal – ferromagnet interface. The denominator \mathcal{D} in Eqs. 28, 29 is

$$\mathcal{D} = X^\uparrow X^\downarrow (\bar{A})^2 [1 - z^2 + (z')^2 + 2iz] + (X^\uparrow Y^\downarrow + X^\downarrow Y^\uparrow)[-z^2 + (z')^2 + iz] + Y^\uparrow Y^\downarrow A^2 [-z^2 + (z')^2].$$

3.2.2 Incoming electron with a spin-down

We now consider an incoming electron with a spin-down while the impurity has initially a spin-up. The wave functions are

$$\hat{\psi}_{i\uparrow}^{e\downarrow}(x) = \begin{pmatrix} 0 \\ 1 \end{pmatrix} e^{ikx} + \begin{pmatrix} b_{i\uparrow}^{e\downarrow \rightarrow e\uparrow} \\ b_{i\uparrow}^{e\downarrow \rightarrow e\downarrow} \end{pmatrix} e^{-ikx} \text{ if } x < 0. \quad (30)$$

$$\hat{\psi}_{i\uparrow}^{e\downarrow}(x) = \begin{pmatrix} \alpha' \\ \alpha \end{pmatrix} e^{ikx} + \begin{pmatrix} \beta' \\ \beta \end{pmatrix} e^{-ikx} \text{ if } 0 < x < a. \quad (31)$$

$$\hat{\psi}_{i\uparrow}^{e\downarrow}(x) = t_{i\uparrow}^{e\downarrow \rightarrow e\downarrow} \begin{pmatrix} 0 \\ 1 \end{pmatrix} e^{ik^\downarrow x} + t_{i\uparrow}^{e\downarrow \rightarrow e\uparrow} \begin{pmatrix} 1 \\ 0 \end{pmatrix} e^{ik^\uparrow x} \text{ if } x > a. \quad (32)$$

It is straightforward to show that the equations for $t_{i\uparrow}^{e\downarrow \rightarrow e\uparrow}$ and $t_{i\uparrow}^{e\downarrow \rightarrow e\downarrow}$ are obtained from the ones in section 3.2.1 under the transformation $A^\uparrow \leftrightarrow A^\downarrow$, and $Z^\uparrow \leftrightarrow Z^\downarrow$. The amplitude for transmission in the ferromagnet is

$$t_{i\uparrow}^{e\downarrow \rightarrow e\uparrow} = -\frac{1}{\mathcal{D}A^\uparrow} iz'[\overline{A}X^\downarrow + AY^\downarrow] \quad (33)$$

$$t_{i\uparrow}^{e\downarrow \rightarrow e\downarrow} = \frac{1}{\mathcal{D}A^\downarrow} [\overline{A}(1 + iz)X^\uparrow + AizY^\uparrow]. \quad (34)$$

3.3 Scattering in the total spin $S^z = \pm 1$ sectors

The incoming electron does not undergo spin-flip scattering in the sectors with a total spin $S^z = \pm 1$. The transmission coefficient in the sector $S^z = 1$ is found to be

$$t_{i\uparrow}^{e\uparrow \rightarrow e\uparrow} = \frac{1}{A^\uparrow[\overline{A}(1 + i(z + z'))X^\uparrow + Aiz(z + z')Y^\uparrow]}. \quad (35)$$

In the sector $S^z = -1$, we have

$$t_{i\downarrow}^{e\downarrow \rightarrow e\downarrow} = \frac{1}{A^\downarrow[\overline{A}(1 + i(z + z'))X^\downarrow + Aiz(z + z')Y^\downarrow]}. \quad (36)$$

We can check easily that these forms of the transmission coefficient are identical to Eq. 28, with $z' = 0$, and the replacement $z \rightarrow z + z'$. This is expected since there is no spin-dependent scattering in the limit $z' = 0$ of Eq. 28.

3.4 Landauer formula

We now evaluate the total conductance and assume that the incoming electron and impurity do not have any preferential direction. The conductance is the sum of four terms, weighted by the probability $\mathcal{P} = 1/2$ to have a spin-up or spin-down impurity: $G = (G_{i\downarrow}^{e\uparrow} + G_{i\uparrow}^{e\downarrow} + G_{i\uparrow}^{e\uparrow} + G_{i\downarrow}^{e\downarrow})/2$, with

$$G_{i\downarrow}^{e\uparrow} = \frac{e^2}{h} \left(\frac{k^\uparrow}{k} |t_{i\downarrow}^{e\uparrow \rightarrow e\uparrow}|^2 + \frac{\text{Re}k^\downarrow}{k} |t_{i\downarrow}^{e\uparrow \rightarrow e\downarrow}|^2 \right) \quad (35)$$

$$G_{i\uparrow}^{e\downarrow} = \frac{e^2}{h} \left(\frac{k^\uparrow}{k} |t_{i\uparrow}^{e\downarrow \rightarrow e\uparrow}|^2 + \frac{\text{Re}k^\downarrow}{k} |t_{i\uparrow}^{e\downarrow \rightarrow e\downarrow}|^2 \right) \quad (36)$$

$$G_{i\uparrow}^{e\uparrow} = \frac{e^2}{h} \frac{k^\uparrow}{k} |t_{i\uparrow}^{e\uparrow \rightarrow e\uparrow}|^2 \quad (37)$$

$$G_{i\downarrow}^{e\downarrow} = \frac{e^2}{h} \frac{\text{Re}k^\downarrow}{k} |t_{i\downarrow}^{e\downarrow \rightarrow e\downarrow}|^2. \quad (38)$$

We have incorporated the possibility of having a pure imaginary wave vector k^\downarrow , corresponding to an empty spin-down band.

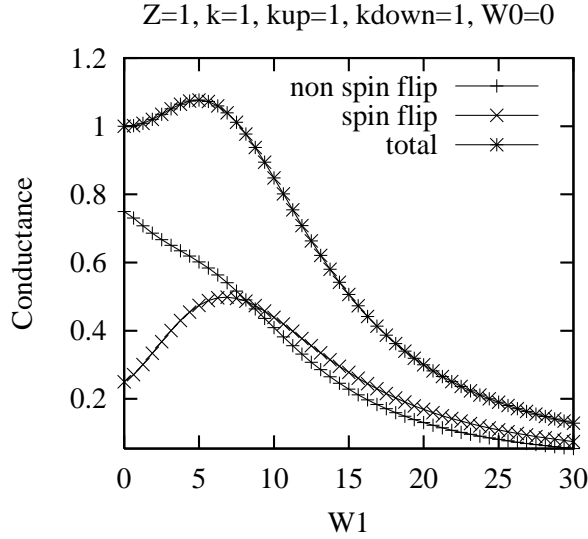


Figure 9: Spin-flip, non spin-flip, and total conductances (in units of e^2/h) of the quantum mechanical toy model of magnetic scattering close to a ferromagnet interface, with an unpolarized ferromagnet ($k = k^\uparrow = k^\downarrow = 1$) and the parameters $Z = 1$, $a = 100$ and $W_0 = V_0/H = 0$. The conductances are plotted as a function of $W_1 = V_1/H$.

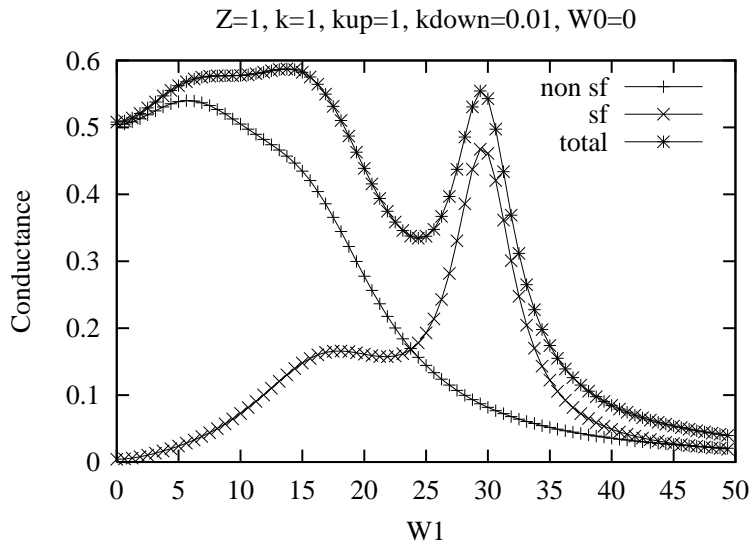


Figure 10: Spin-flip, non spin-flip, and total conductances (in units of e^2/h) of the quantum mechanical toy model of magnetic scattering close to a ferromagnet interface, with a strongly polarized ferromagnet ($k = k^\uparrow = 1, k^\downarrow = 0.01$) and the parameters $Z = 1$, $a = 100$ and $W_0 = V_0/H = 0$. The conductances are plotted as a function of $W_1 = V_1/H$. A resonance, not present on Fig. 9, develops in the conductance upon spin polarizing the ferromagnet.

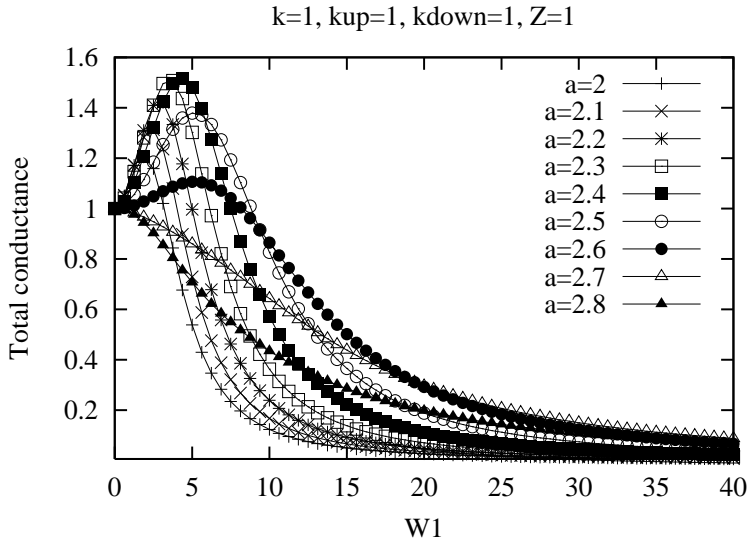


Figure 11: Total conductance (in units of e^2/h) of the spin-flip Fabry-Perot interferometer, in the unpolarized case $k = k^\uparrow = k^\downarrow = 1$, and with $Z = 1$, $W_0 = 0$. The conductances are plotted as a function of $W_1 = V_1/H$. The different curves correspond to different values of $a = 2, 2.1, 2.2, 2.3, 2.4, 2.5, 2.6, 2.7, 2.8$.

3.5 Magnetic proximity effect

To mimic the effect of diffusion, we consider the presence of a strong interface scattering at the metal – ferromagnet interface, with the parameter $Z = 1$. The electron are multiply reflected before they enter the ferromagnet, and we first choose the parameter a in such a way that spin-flip scattering is resonant. As it is visible on Figs. 9 and 10, the presence of a spin polarization in the ferromagnet generates a peak in the conductance, not present in the unpolarized situation. This resonance originates solely from the spin-flip contribution of the conductance.

On the other hand, Figs. 9, 10 have been obtained for a specific value of the distance a between the impurity and the ferromagnet interface such that the system was resonant. We have plotted on Figs. 11 and 12 the variations of the total conductances for different values of the parameter a . The peak in the conductance of the polarized ferromagnet model appears to be a resonance of the spin-flip Fabry Perot interferometer model.

4 Conclusions

To conclude, we have studied the possibility of a magnetic proximity effect, induced by spin-flip scattering in a diffusive wire in contact with two ferromagnets with an antiparallel magnetization. With a sufficient spin polarization, the conductance of this type of junction increases with the amount of spin-flip scattering, or equivalently, with the resistance of the diffusive wire. We have shown that

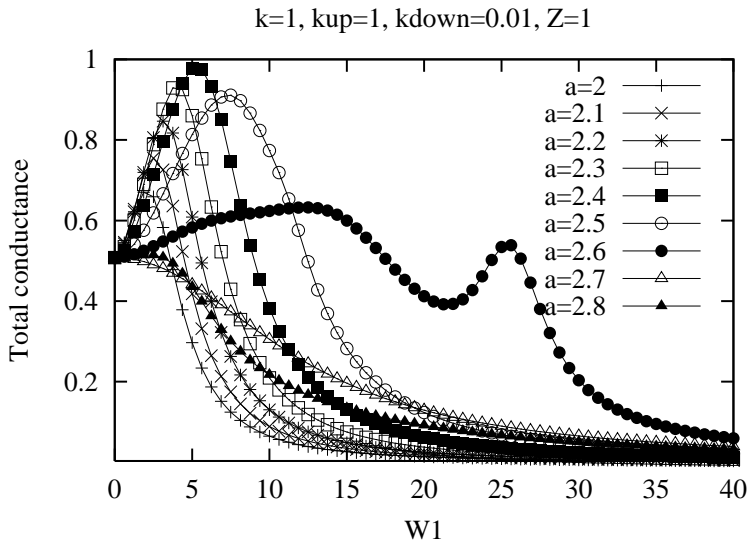


Figure 12: Total conductance (in units of e^2/h) of the spin-flip Fabry-Perot interferometer, in the spin polarized case $k = k^\uparrow = 1$, $k^\downarrow = 0.01$, and with $Z = 1$, $W_0 = 0$. The conductances are plotted as a function of $W_1 = V_1/H$. The different curves correspond to different values of $a = 2, 2.1, 2.2, 2.3, 2.4, 2.5, 2.6, 2.7, 2.8$. Notice the presence of a resonance for $a = 2.6$, not present for the unpolarized model (see Fig. 11).

this type of physics appears for strongly polarized magnets. A similar physics also exists for a diffusive wire in contact with a normal metal and a ferromagnet, on the condition that the contacts have a low transparency. We have also studied a quantum mechanical “spin-flip Fabry Perot” model in which phase coherent multiple scatterings are treated on a rigorous basis. In this model, the magnetic proximity effect appears as a resonance in the spin-flip channels.

The effect of spin-flip scattering as been studied in the context of GMR [17, 18]. This problematics is not far from what we have considered in the present work, except that we have carried out a precise analysis of the dependence of the conductance upon the length of the diffusive wire, pointed out the analogy with the superconducting proximity effect, and analyzed the relation with a model for quantum coherent scattering. We have considered here only the effect of a surface scattering. A more realistic model would involve the treatment of spin-dependent bulk scattering in the ferromagnets as well, with a spin-up diffusion coefficient smaller than the spin-down diffusion coefficient. Qualitatively, we expect the same physics for bulk and surface scattering. In the case of bulk scattering, and in the antiparallel alignment, minority spin electrons are injected into one of the ferromagnets, with a large diffusion constant. In the presence of spin-flip scattering in the intermediate wire, these electrons can change their spin and enter the ferromagnet as a majority spin. Therefore, spin-flip scattering in the intermediate wire should also increase the conductance.

A possibility to test in an experiment the type of magnetic proximity effect considered in this work

would consist in realizing a mesoscopic system, with a diffusive region connected to two ferromagnets. The diffusive region may be intentionally doped with magnetic impurities and the conductance would increase linearly with the doping concentration. The conductance in the proximity effect regime would also decrease with a decreasing temperature. Another possible experiment would be to use a SQUID magnetometry to measure the magnetization induced in the normal wire. This could be done with a single ferromagnet connected to a wire doped with magnetic impurities. The induced magnetic moment could be monitored by the applied voltage. Finally, we have considered here a one dimensional wire connected to ferromagnetic reservoirs. We expect an identical physics in the case of a three dimensional conductor connected to ferromagnetic reservoirs.

A Derivation of the Boltzmann equation with spin-flip scattering

We give a brief derivation of the Boltzmann equation Eq. 1 in the presence of a spin-flip scattering potential. The derivation generalizes Ref. [34] to incorporate a spin-flip scattering self energy. The Dyson equation in the spin tensor Keldysh space reads $(\hat{G}_0^{-1} - \hat{\Sigma})(1, 2) \otimes \hat{G}(2) = \delta(1 - 2)$. The convolution includes a sum over coordinates, time, and spin. The kinetic equation is obtained from the difference of the Keldysh components of the Dyson equations and its conjugate:

$$[\hat{G}_0^{-1} - \text{Re}\hat{\Sigma}, \hat{G}^K]_- - [\hat{\Sigma}^K, \text{Re}\hat{G}]_- = \frac{i}{2} [\hat{\Sigma}^K, \hat{A}]_+ - \frac{i}{2} [\hat{\Gamma}, \hat{G}^K]_+, \quad (39)$$

with $[\cdot]_-$ and $[\cdot]_+$ denoting a commutator and an anticommutator respectively. We refer the reader to Ref. [34] for an explanation of the symbols used in Eq. 39. We use the the self energy shown on Fig. 13:

$$\hat{\Sigma}_\sigma(\mathbf{p}, \mathbf{R}, T) = n_i \int \frac{d\mathbf{p}'}{(2\pi)^3} |v(\mathbf{p} - \mathbf{p}')|^2 \hat{G}_{\sigma,\sigma}(\mathbf{p}', \mathbf{R}, T) + n'_i \int \frac{d\mathbf{p}'}{(2\pi)^3} |v'(\mathbf{p} - \mathbf{p}')|^2 \hat{G}_{-\sigma,-\sigma}(\mathbf{p}', \mathbf{R}, T), \quad (40)$$

with n_i and n'_i the concentration of non magnetic and magnetic impurities. The first term in Eq. 40 describes non spin-flip scattering, and the second term describes spin-flip scattering. Notice that this self energy does not incorporate the Kondo effect since we do not incorporate the possibility of a having hole in the intermediate state.

We assume the self energy in Eq. 39 to be constant in space, and use the gradient expansion to first order

$$(A \otimes B)_{\sigma,\sigma'}(X, p) \simeq \sum_{\sigma_2} \left[1 + \frac{i}{2} \left(\partial_X^A \partial_p^B - \partial_p^A \partial_X^B \right) \right] A_{\sigma,\sigma_2} B_{\sigma_2,\sigma'}.$$

If A and B are symmetric in spin $A_{\sigma,\sigma'} = A_{\sigma',\sigma}$, and $B_{\sigma,\sigma'} = B_{\sigma',\sigma}$, the commutator reduces to the usual spinless Poisson bracket: $[A \otimes B]_{-\sigma,\sigma'} = i \sum_{\sigma_2} \{A_{\sigma,\sigma_2}, B_{\sigma_2,\sigma'}\}$, with $\{A, B\} = \partial_X^A A \partial_p^B B - \partial_p^A A \partial_X^B B$. Using these relations, we expand the kinetic equation Eq. 39 and integrate over energy to obtain the Boltzmann equation

$$\partial_T f_{\mathbf{p},\sigma} + \nabla_{\mathbf{p}} \xi_{\mathbf{p}} \nabla_{\mathbf{R}} f_{\mathbf{p},\sigma} - \nabla_{\mathbf{R}} U \nabla_{\mathbf{p}} f_{\mathbf{p},\sigma} = 2\pi n_i \int \frac{d\mathbf{p}'}{(2\pi)^3} |v(\mathbf{p} - \mathbf{p}')|^2 \delta(\xi_{\mathbf{p}} - \xi_{\mathbf{p}'}) [f_{\mathbf{p}',\sigma} - f_{\mathbf{p},\sigma}] \quad (41)$$

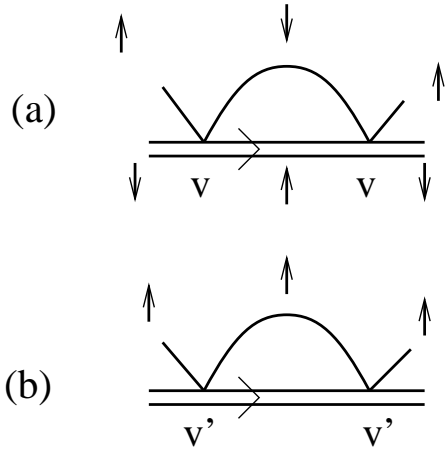


Figure 13: The self energy terms incorporated in the gradient expansion calculation. The term shown on Fig. 8 (b) generating the Kondo effect is not included.

$$+2\pi n'_i \int \frac{d\mathbf{p}'}{(2\pi)^3} |v'(\mathbf{p} - \mathbf{p}')|^2 \delta(\xi_{\mathbf{p}} - \xi_{\mathbf{p}'}) [f_{\mathbf{p}', -\sigma} - f_{\mathbf{p}, \sigma}].$$

In the one dimensional limit, Eq. 41 reduces to the Boltzmann equation Eq. 1, with the scattering coefficients related to the $q = 0$ and $q = 2k_f$ components of the scattering potential: $r = n_i |v_{2k_f}|^2$, $r_s = n'_i |v_0|^2$, and $r'_s = n'_i |v'_{2k_f}|^2$.

References

- [1] M.J. Zuckermann, Solid State Commun. **12**, 745 (1973).
- [2] B.N. Cox, R.A. Tehir-Kheli, and R.J. Elliott, Phys. Rev. B **20**, 2864 (1979).
- [3] J. Tersoff and L.M. Falicov, Phys. Rev. B **26**, 6186 (1982).
- [4] R.M. White and D.J. Friedman, J. Magn. Mater. **49**, 117 (1985).
- [5] L. Libermann, J. Clinton, D.M. Edwards, and J. Mathin, Phys. Rev. Lett. **25**, 232 (1970).
- [6] G. Bergmann, Phys. Rev. Lett. **41**, 264 (1978); Physics Today **32**, 25 (1979).
- [7] K.M. Gyorgy, J.F. Dillon, D.B. Mcwhan, L.W. Rupp, and L.R. Testardi, Phys. Rev. Lett. **45**, 5151 (1980).
- [8] J.S. Moodera, M.E. Taylor, and R. Meservey, Phys. Rev. B **40**, 11980 (1984).
- [9] A. Frydman and R.C. Dynes, Report No cond-mat/9810061.
- [10] P.G. de Gennes, *Superconductivity of metals and alloys*, W.A. Benjamin, New York (1966); reprinted by Addison-Wesley, Reading, MA (1989).
- [11] F.W.J. Hekking and Yu. V. Nazarov, Phys. Rev. Lett. **71**, 1625 (1993).
- [12] *The Kondo Problem to Heavy Fermions*, A.C. Hewson, Cambridge Studies in Magnetism, Cambridge University Press (1993).
- [13] T. Valet and A. Fert, Phys. Rev. B **48**, 7099 (1993).
- [14] K.M. Schep, J.B.A.N. van Hoof, P.J. Kelly, G.E.W. Bauer, and J.E. Inglesfield, J. Magn. Magn. Mater. **177**, 1166 (1998).
- [15] S. Zhang and P.M. Levy, Phys. Rev. B **57**, 5336 (1998).
- [16] M.D. Stiles and D.R. Penn, Phys. Rev. B **61**, 3200 (2000).
- [17] R.Y. Gu, D.Y. Xing, and Z.D. Wang, Phys. Rev. B **58**, 11142 (1998).
- [18] J. Chen and S. Hershfield, Phys. Rev. B **57**, 1097 (1998).
- [19] V.I. Kozub and A.M. Rudin, Phys. Rev. B **52**, 7853 (1995).
- [20] K.E. Nagaev, Phys. Rev. B **52**, 4740 (1995).
- [21] G.E. Blonder, M. Tinkham, and T.M. Klapwijk, Phys. Rev. B **25**, 4515 (1982).

- [22] M.J.M. de Jong, Phys. Rev. B **49**, 7778 (1994).
- [23] Yu. Nazarov and T.H. Stoof, Phys. Rev. Lett. **76**, 823 (1996).
- [24] C.W.J. Beenakker, Rev. Mod. Phys. **69**, 731 (1997).
- [25] A.F. Volkov, A.V. Zaitsev, and T.M. Klapwijk, Physica C **210**, 21 (1993).
- [26] A.V. Zaitsev, Phys. Lett. A **194**, 315 (1994).
- [27] V.T. Petrashov, V.N. Antonov, P. Delsing, and R. Claeson, Phys. Rev. Lett. **70**, 347 (1993).
- [28] H. Courtois, Ph. Gandit, D. Mailly, and B. Pannetier, Phys. Rev. Lett. **76**, 130 (1996).
- [29] P. Charlat, H. Courtois, Ph. Gandit, D. Mailly, A.F. Volkov, and B. Pannetier, Phys. Rev. Lett. **77**, 4950 (1996).
- [30] W. Belzig, C. Bruder, and G. Schön, Phys. Rev. B **54**, 9443 (1996).
- [31] H. Pothier, S. Guéron, D. Esteve, and M. H. Devoret, Phys. Rev. Lett. **73**, 2488 (1994).
- [32] S. Guéron, H. Pothier, N.O. Birge, D. Esteve, and M.H. Devoret, Phys. Rev. Lett. **77**, 3025 (1996).
- [33] J.X. Zhu and Z.D. Wang, Phys. Rev. B **55**, 8437 (1997).
- [34] J. Rammer and H. Smith, Rev. Mod. Physics **58**, 323 (1986).